

## Stabilization of $\alpha$ -Helices by Dipole–Dipole Interactions within $\alpha$ -Helices

Changmoon Park<sup>†</sup> and William A. Goddard III\*

Materials and Process Simulation Center, Beckman Institute (139-74), Division of Chemistry and Chemical Engineering, California Institute of Technology, Pasadena, California 91125

Received: January 13, 2000; In Final Form: May 16, 2000

Including solvation effects (in the Poisson–Boltzmann continuum solvent approximation) we report ab initio quantum mechanical calculations (HF/6-31G\*\*) on the conformational energies for adding alanine to the amino or carboxyl terminus of a polyalanine  $\alpha$ -helix as a function of helix length  $N$ . We find that extending the length of an  $\alpha$ -helix increasingly favors the  $\alpha$ -helix conformation for adding an additional residue, even in hydrophobic environment. Thus,  $\alpha$ -helix formation is a cooperative process. Using charges from the QM calculations, we find that the electrostatic energy dominates the QM results, showing that this increasing preference for  $\alpha$ -helix formation results from dipole–dipole interaction within the  $\alpha$ -helix. These results provide quantitative preferences and insight into the conformational preferences and kinetics of protein folding.

### 1. Introduction

To carry out directed design of new proteins with designed properties, it is important to understand the determinants of the structure and properties of natural proteins.<sup>1–3</sup> In particular, we need to understand the relation between the sequence and the kinetics of protein folding to understand how the primary sequence of amino acids influences the native structure of a protein.<sup>4–7</sup> Hierarchical procedures using the primary sequence of a protein to reduce the number of plausible conformations of a protein are essential to reduce the number of conformations to a level that can be rapidly analyzed by the modern computers and methods.<sup>8,9</sup> Since 70% of protein structures consist of specific secondary structures (mostly  $\alpha$ -helix,  $\beta$ -sheets, and turns), the ability to predict secondary structures is essential to predicting the tertiary structures of proteins, and many methods have been developed starting with the Chou and Fasman analysis of secondary structure preferences.<sup>10–13</sup> The current state of the art is incorporated in PhD<sup>14</sup> (see also ref 15 for review).

Many good model systems have been developed for understanding the  $\alpha$ -helix secondary structures of proteins.<sup>16,17</sup> The formation of the first turn of an  $\alpha$ -helix was shown to be rate-determining in the formation of the whole  $\alpha$ -helices.<sup>18</sup> After formation of this first turn, the growth process of  $\alpha$ -helix elongation is fast and cooperative,<sup>19–21</sup> leading to  $\alpha$ -helix formation in nanosecond time scales.<sup>21,22</sup>

The parallel alignment of both the amino (NH) and carbonyl (CO) groups of each residue constituting an  $\alpha$ -helix leads to a net dipole moment (the macrodipole) with the partial positive charge at its N-terminus and the partial negative charge at its C-terminus.<sup>23,24</sup> The interactions between the dipole moments of the  $\alpha$ -helix with dipolar or charged groups located at the ends have been studied experimentally,<sup>25–27</sup> showing that these interactions help stabilize dipolar groups through dipole–dipole interactions and stabilize charged groups through dipole-charge interactions, with the former less screened by solution effects. However, there has been less attention paid to the interactions occurring *within* the macrodipole of  $\alpha$ -helices (Figure 1).<sup>28,29</sup>

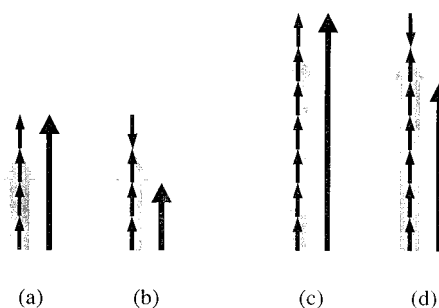


**Figure 1.** Schematic diagram for the monodipole–macro-dipole interactions. The small black arrow indicates the dipole of each alanine monomer (monodipole), the big gray arrow indicates the total dipole moment of the  $\alpha$ -helix (macro-dipole) in which the one alanine at the N-terminus is excluded while the long black arrow indicates the resulting total dipole moment of the  $\alpha$ -helix. As indicated by the orientation of the dipole moment vector, the N-termini are positive (at the top) while the C-termini are negative (at the bottom). (a)  $(Ala)_4_N\alpha$ ; a 4-alanine peptide in which all alanines are in the  $\alpha$ -helical conformations ( $\phi = -57^\circ$ ,  $\psi = -47^\circ$ ). (b)  $(Ala)_4_Np\beta$  or  $(Ala)_4_Na\beta$ ; the same as  $(Ala)_4_N\alpha$  except the alanine at the N-terminus is in its parallel  $\beta$ -sheet ( $\phi = -119^\circ$ ,  $\psi = 113^\circ$ ) or antiparallel  $\beta$ -sheet ( $\phi = 139^\circ$ ,  $\psi = 135^\circ$ ) conformation. (c)  $(Ala)_7_N\alpha$ . (d)  $(Ala)_7_Np\beta$  or  $(Ala)_7_Na\beta$ .

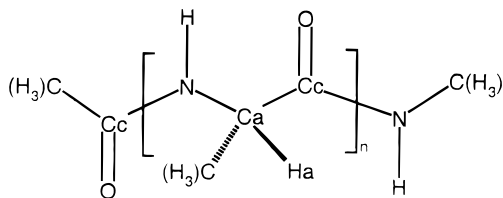
Gas-phase quantum mechanical (QM) calculations have suggested that the right-handed  $\alpha$ -helical conformation is *not* a stable structure because the dipole moment of each residue is located in an unfavorable orientation with each other.<sup>29,30</sup> However, we find that including solvation accurately in the QM calculations favors stabilizing the  $\alpha$ -helical conformation with respect to the  $\beta$ -sheet conformation.<sup>31</sup>

On the other hand, most  $\alpha$ -helices found in the X-ray crystal structures of proteins are in hydrophobic regions (even the amphiphilic  $\alpha$ -helices aggregate in water to avoid exposing the hydrophobic face to solvent). This implies that  $\alpha$ -helices can form in hydrophobic environments.

To learn how this occurs we carried out QM calculations on polyalanine peptides to study factors stabilizing and determining  $\alpha$ -helical conformations even in hydrophobic environment. We find that monodipole–macro-dipole interactions within an  $\alpha$ -helix (see Figure 1) increasingly stabilizes longer  $\alpha$ -helices.

\* To whom correspondence should be addressed (wag@wag.caltech.edu).

<sup>†</sup> Permanent address: College of Natural Sciences, Department of Chemistry, Chungnam National University, Taejeon, South Korea 305-764.

**TABLE 1: Geometric Data Parameters Used for the Polyalanine**

bond	length (Å)	bond	length (Å)
N–H	1.08	Cc–O	1.24
N–Ca	1.46	Cc–N	1.32
Ca–C(H3)	1.54	N–C(H3)	1.46
Ca–Ha	1.11	Cc–C(H3)	1.51
Ca–Cc	1.51		
bond	angle (deg)	bond	angle (deg)
(H3)C–Cc–O	122.0	N–Ca–Cc	111.0
(H3)C–Cc–N	116.0	Ca–Cc–O	122.0
Cc–N–H	116.0	Ca–Cc–N	116.0
Cc–N–Ca	122.0	Cc–N–H	116.0
N–Ca–C(H3)	107.6	Cc–N–C(H3)	122.0
N–Ca–Ha	108.6		
bond	torsion angle (deg)	bond	torsion angle (deg)
(H3)C–Cc–N–H	0.0	N–Ca–Cc–O	133.6
(H3)C–Cc–N–Ca	180.0	N–Ca–Cc–N	$\Psi^*$
Cc–N–Ca–C(H3)	109.1	Ca–Cc–N–H	0.0
Cc–N–Ca–Ha	60.7	Ca–Cc–N–C(H3)	180.0
Cc–N–Ca–Cc	$\Phi^*$		

\* Indicate two  $\Phi$  and  $\Psi$  torsional angles.

Section 2 discusses the methods and section 3 describes the results. On the basis of these results section 4 discusses the folding mechanism of  $\alpha$ -helix formation.

## 2. Calculation Methods

The calculations considered only polyalanine peptides,  $\text{CH}_3\text{CO}-(\text{Ala})_N\text{-NHCH}_3$ , in which the N- and C-termini were neutralized by adding  $\text{CH}_3\text{CO}-$  and  $-\text{NHCH}_3$  groups, respectively. This avoids extra charges that might play a role at the amino and carboxyl termini. The notational and geometry information for the polyalanine peptides are shown in Figure 1 and Table 1, respectively

**2.1. QM Calculations.** All QM calculations were at the Hartree–Fock (HF) level using the 6-31G\*\* basis for all atoms (using the Jaguar 3.5 quantum chemistry program).<sup>32,33</sup> Solvation was included using the Poisson–Boltzmann continuum model (PBF) with a realistic molecular surface (van der Waals radius plus solvent radius about each atom)<sup>34</sup> in Jaguar 3.5 from Schrodinger. We used a dielectric constant for water of 80.37 and a probe radius of 1.4 Å for water. At each iteration, the wave function is calculated self-consistently in the field of the solvent and then the charges (based on the electrostatic potential from the HF wave function) are used to calculate a new reaction field. This process is repeated until convergence. The solvent reaction field is updated at each SCF step.

**2.2. Conformational Maps.** We examined the dipole–macro-dipole interactions between the dipole moment (monodipole) of the alanine at the amino terminus (as a function of conformation) and the macrodipole of the  $N - 1$   $\alpha$ -helix residues (Figure 1) using QM with solvation. To study the length dependence of the monodipole–macro-dipole interaction within  $\alpha$ -helix, we carried out QM calculations for  $(\text{Ala})_4\text{N}$ , a 4-alanine peptide in which all alanines are in the  $\alpha$ -helical conformation except the alanine at the N-terminus can be in

any conformation. We also carried out QM calculations for  $(\text{Ala})_7\text{N}$ , the same as  $(\text{Ala})_4\text{N}$  except a 7-alanine peptide. To determine the effect of  $\alpha$ -helix length on the monodipole–macro-dipole interaction, the difference between the QM results for  $(\text{Ala})_4\text{N}$  and  $(\text{Ala})_7\text{N}$  were calculated. To extract the pure effect of the three alanines added at the C-terminus of the  $(\text{Ala})_4\text{N}$  to make  $(\text{Ala})_7\text{N}$ , all alanines except the one on the amino terminus were kept in the  $\alpha$ -helical conformation for all calculations

The QM calculations were carried out for torsional angles of  $\phi = -180^\circ$  to  $0^\circ$  and  $\psi = -180^\circ$  to  $180^\circ$  with increments of  $60^\circ$ . This leads to 24 points. We calculated 16 additional points to improve the contour around the  $\alpha$ -helix and  $\beta$ -sheet conformations. Here we considered the torsional angles of  $\phi = -30^\circ$  to  $-90^\circ$  and  $\psi = -150^\circ$  to  $-90^\circ$ , and  $\phi = -90^\circ$  to  $-150^\circ$  and  $\psi = 90^\circ$  to  $150^\circ$ , respectively. We also considered three additional conformations corresponding to  $\alpha$ -helix ( $\phi = -57^\circ$  and  $\psi = -47^\circ$ ), parallel  $\beta$ -sheet ( $\phi = -119^\circ$  and  $\psi = 113^\circ$ ), and antiparallel  $\beta$ -sheet ( $\phi = -139^\circ$  and  $\psi = 135^\circ$ ). For the energy maps (Figures 2 and 3) the geometry of each conformation (Table 1) was created using the amino acid building model from Insight.<sup>35</sup> The geometries were *not* optimized at this point so that we could study the pure effects of the dipole–macro-dipole interaction according to the relative orientation of the dipole moment of the added alanine to the macrodipole of the original  $\alpha$ -helices.

The same calculations were carried out for monodipole–macro-dipole interactions between the alanine at the carboxyl terminus and the macrodipole of the  $N - 1$   $\alpha$ -helix residues (Figure 4).

**2.3. MM Calculations.** To interpret the QM conformational energy surface in terms of electrostatic interactions, we carried out classical electrostatic energy calculations using the ESP derived point charges from the QM calculations. The bonds, angles, torsions, and all the other force field terms were *turned off*. ESP derived charges are sensitive to conformational changes. We tested the two cases with the two set of ESP derived charges as shown in Table 2: (i) all N alanines in the  $\alpha$ -helical conformation and (ii) the N-terminus in the  $\beta$ -sheet conformation but the remaining  $N - 1$  residues in the  $\alpha$ -helical conformation.

We used the MM electrostatic energies to compare with the results of QM calculations (Table 2). (Other details of the MM calculations are in the caption of Table 2.) We found that MM electrostatic energy difference for  $\alpha$ -helix versus  $\beta$ -sheet matches well the QM difference.

**2.4. Optimized Structures for  $\alpha$ -Helix and  $\beta$ -Sheet Amino Terminus.** To determine the length dependence of differential energy stabilization for the alanine at the N-terminus (and C-terminus) of an  $\alpha$ -helix, we carried out QM calculations for polyalanine peptides for various lengths of  $\alpha$ -helices. In these calculations, the geometry was completely optimized quantum mechanically but with the appropriate torsional angle constraints for all residues. The QM calculations were done both in gas phase and solvated in water (Figure 5, Table 3).

## 3. Results

**3.1. Conformational Maps.** *3.1.1. QM Results.* Figure 2 shows the results of QM calculations for various  $\phi$  and  $\psi$  torsional angles of the added alanine at the N-terminus while the structure of the remaining residues is kept fixed in an  $\alpha$ -helix. The maps are qualitatively similar to those for the Gly-Ala-Gly tripeptide in our previous calculations (Figure 2 in ref 31), but the depth of the minima and the height of the maxima are different. These results show clearly that adding alanine to

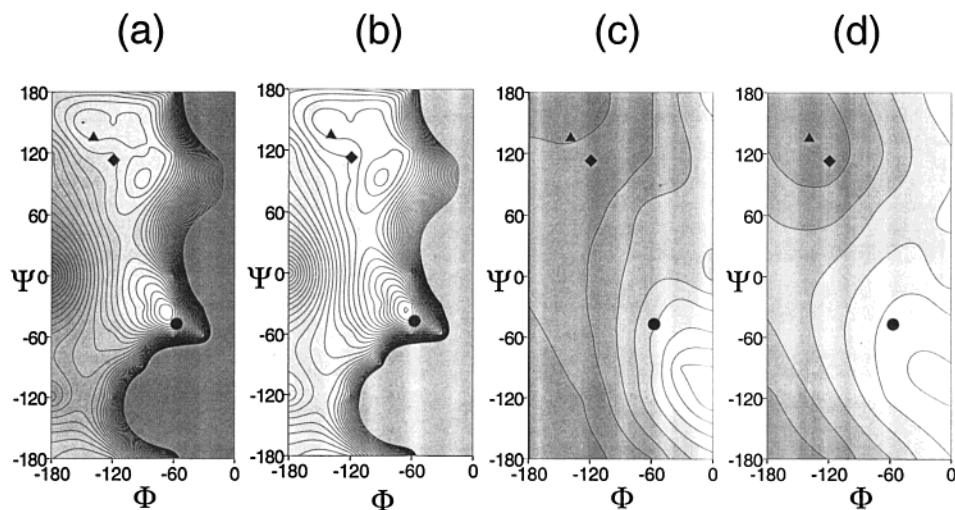


**Figure 2.** Conformational surfaces for the amino terminus of (Ala)<sub>4</sub>\_N and (Ala)<sub>7</sub>\_N from gas-phase HF/6-31G\*\* calculations. In each case all alanines were kept in the  $\alpha$ -helix conformation except the N-terminus. Each map is based on the energies for 40 pairs of torsional angles [24 from ( $\delta\phi = 60^\circ$ ,  $\delta\psi = 60^\circ$ ) and 16 from ( $\delta\phi = 30^\circ$ ,  $\delta\psi = 30^\circ$ ), 8 of which are centered at each of ( $\phi = -120^\circ$ ,  $\psi = 120^\circ$ ) and ( $\phi = -60^\circ$ ,  $\psi = -60^\circ$ )] plus three additional energies corresponding to the  $\alpha$ -helix ( $\phi = -57^\circ$ ,  $\psi = -47^\circ$ ; indicated by  $\bullet$ ) the parallel  $\beta$ -sheet ( $\phi = -119^\circ$ ,  $\psi = 113^\circ$ ; indicated by  $\blacklozenge$ ), and the antiparallel  $\beta$ -sheet ( $\phi = -139^\circ$ ,  $\psi = 135^\circ$ ; indicated by  $\blacktriangle$ ) conformations. The bright region indicates stable conformations and the dark region indicates unstable conformations. The contour spacing is 1.0 kcal/mol. (a) The total energy of gas phase (Ala)<sub>4</sub>\_N (the absolute minimum in water is near the  $\alpha$ -helix while a second minima near the  $\beta$ -sheet position is  $\sim 4$  kcal/mol higher). (b) The total energy for gas phase (Ala)<sub>7</sub>\_N (the absolute minimum in water is the  $\alpha$ -helix while a second minimum is near the  $\beta$ -sheet position is  $\sim 7$  kcal/mol higher). (c) The energy difference between gas phase (Ala)<sub>4</sub>\_N and (Ala)<sub>7</sub>\_N. (d) The total dipole moment of gas phase (Ala)<sub>7</sub>\_N (the value near the  $\alpha$ -helix is 32.3 D while the values near the  $\beta$ -sheet are 24.2 and 23.5 D). The contour spacing is 2.0 D.

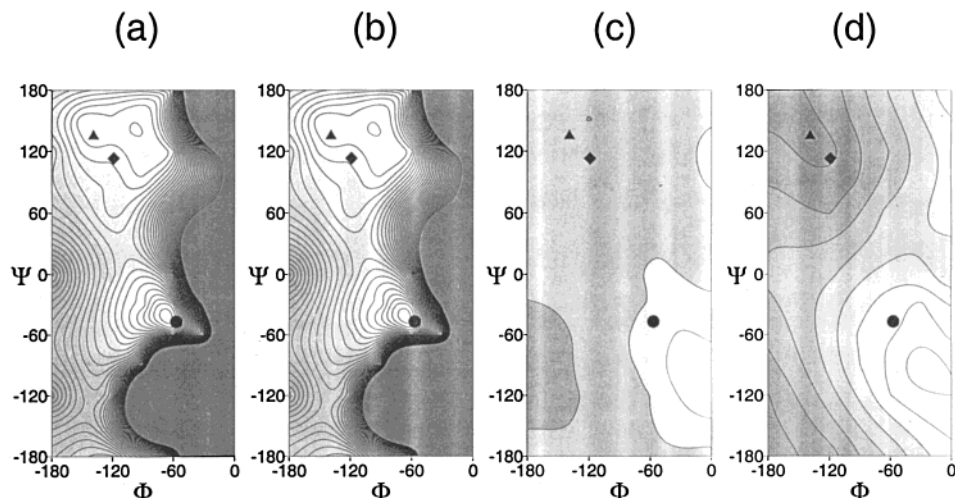


**Figure 3.** Same as for Figure 2 except solution phase results.

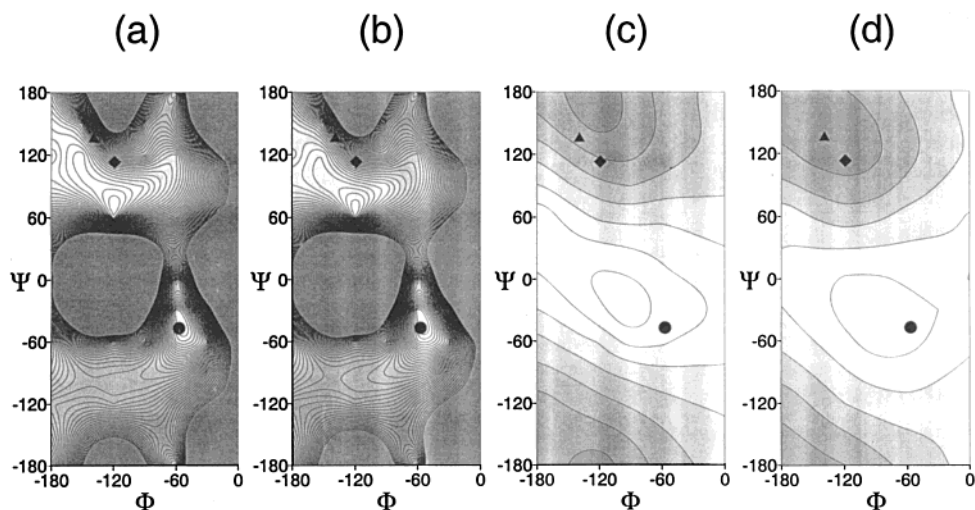
the amino terminus of an  $\alpha$ -helix leads to distinct minima at the  $\alpha$ -helical and  $\beta$ -sheet conformations.

Figure 2a shows that adding alanine to (Ala)<sub>3</sub> in the  $\alpha$ -helical conformation is  $\sim 3$  kcal/mol more stable than adding it in the  $\beta$ -sheet conformation. This differential preference for the  $\alpha$  conformation increases as the length of  $\alpha$ -helix becomes longer. Thus, Figure 2b shows that adding alanine to (Ala)<sub>6</sub> leads to stabilization of  $\alpha$  versus  $\beta$  by  $\sim 6$  kcal/mol. This differential effect is shown in Figure 2c, which shows that adding three alanines [going from (Ala)<sub>4</sub> to (Ala)<sub>7</sub>] increases the stabilization of  $\alpha$  by over 3 kcal/mol. Figure 2d shows the magnitude of the dipole moments of (Ala)<sub>7</sub> for various conformations. The similarity with Figure 2c suggests that electrostatic interactions within the  $\alpha$ -helix are the source of this stabilization. In solution, however, this stabilization decreases substantially because of the screening by the water solvent (Figure 3). Compared to the case of (Ala)<sub>4</sub>, the larger dipole moment of (Ala)<sub>7</sub> leads to larger

solvation energy, but this screens the monopole–macro-dipole interaction more effectively.

There are two absolute minima for the conformations of the alanine added at the carboxyl terminus, near ( $\phi = -120^\circ$  and  $\psi = 60^\circ$ ) and  $\alpha$ -helix. For (Ala)<sub>4</sub> the minimum near  $\alpha$ -helix conformation has 0.25 kcal/mol lower energy than the one near ( $\phi = -120^\circ$  and  $\psi = 60^\circ$ ), which increases to 1.83 kcal/mol for (Ala)<sub>7</sub>. Unlike at the amino terminus, the  $\beta$ -sheet conformations are not minima at the carboxyl terminus. However, the results (Figure 4) show that the same trend occurs at the carboxyl terminus. Figure 4c shows that adding three alanines [going from (Ala)<sub>4</sub> to (Ala)<sub>7</sub>] increases the stabilization of  $\alpha$  versus  $\beta$  by over 4 kcal/mol. The similarity between Figure 4c,d also suggests that electrostatic interactions within the  $\alpha$ -helix are the source of this stabilization.

**3.1.2. MM Results.** To measure the role of electrostatic interactions we carried out MM electrostatic energy calculations on the secondary structures of (Ala)<sub>4</sub> and (Ala)<sub>7</sub>. Table 2 shows



**Figure 4.** Same as for Figure 2 except at the carboxyl terminus. In (a) for  $(\text{Ala})_4\text{-C}$ , the energy for the minimum near  $\alpha$ -helix conformation is 0.25 kcal/mol lower than the one near  $(\phi = -120^\circ$  and  $\psi = 60^\circ)$ , which increases to 1.83 kcal/mol in (b) for  $(\text{Ala})_7\text{-C}$  accounting the effect of three alanines added at the amino terminus in (a).

**TABLE 2: Comparison of Gas Phase Energies for the Amino Terminus Alanine Having an  $\alpha$ -Helix or  $\beta$ -Sheet Conformation<sup>a</sup>**

a. Absolute Energies						
	$(\text{Ala})_7\text{-N}$			$(\text{Ala})_4\text{-N}$		
	QM <sup>d</sup>	MM <sup>b</sup>	MM <sup>c</sup>	QM <sup>d</sup>	MM <sup>b</sup>	MM <sup>c</sup>
$E_\alpha$	0.00	20.26	16.67	0.00	6.16	0.99
$E_{\text{p}\beta}$	8.00	29.26	28.58	4.40	12.06	9.69
$E_{\text{a}\beta}$	6.78	27.58	27.25	2.83	10.84	8.64
b. Relative Energies						
	$(\text{Ala})_7\text{-N}$			$(\text{Ala})_4\text{-N}$		
	QM	MM <sup>b</sup>	MM <sup>c</sup>	QM	MM <sup>b</sup>	MM <sup>c</sup>
$dE_{(\alpha\text{-p}\beta)}$	-8.00	-9.01	-11.92	-4.40	-5.90	-8.70
$dE_{(\alpha\text{-a}\beta)}$	-6.78	-7.33	-10.58	-2.83	-4.68	-7.65
c. $E[(\text{Ala})_7\text{-N}] - E[(\text{Ala})_4\text{-N}]$ : Differential Energies Relative to $\text{N}\alpha$						
	QM	MM <sup>b</sup>	MM <sup>c</sup>			
$ddE_{(\alpha\text{-p}\beta)}$	-3.60	-3.11	-3.22			
$ddE_{(\alpha\text{-a}\beta)}$	-3.96	-2.65	-2.93			

<sup>a</sup> Table 2a gives the total QM energy but only the electrostatic energy from the MM electrostatic energy calculations. Table 2b gives the differential between the  $\alpha$ -helix and  $\beta$ -sheet. Table 2c gives the difference between  $N = 4$  and  $N = 7$ . This shows that the QM results are dominated by the electrostatic interactions. <sup>b</sup> The MM calculations used QM charges<sup>e</sup> with the alanine at the N-terminus using torsional angles of  $(\phi = -60^\circ$  and  $\psi = -60^\circ)$ . <sup>c</sup> The MM calculations used QM charges<sup>e</sup> with the alanine at the N-terminus using torsional angles of  $(\phi = -120^\circ$  and  $\psi = 120^\circ)$ . <sup>d</sup> This gives the relative energies to that of  $(\text{Ala})_7\text{-N}\alpha$  or  $(\text{Ala})_4\text{-N}\alpha$ . The total energy of  $(\text{Ala})_7\text{-N}\alpha$  is  $-1967.958900$  hartree while that of  $(\text{Ala})_4\text{-N}\alpha$  is  $-1230.395108$  hartree. <sup>e</sup> The charges are derived based on the electrostatic potential from the HF wave function with the dipole moment constrained to match the QM.

that the electrostatic energies dominate the conformational preferences. Using QM charges from the  $(\phi = -60^\circ$  and  $\psi = -60^\circ)$  conformation, the electrostatic energy difference between  $\alpha$  and  $\beta$  from the MM calculations is comparable (0.5–1.0 kcal/mol larger) to the QM energy. Indeed, the differential stability for  $(\text{Ala})_4$  to  $(\text{Ala})_7$  is also comparable (0.4–1.3 kcal/mol smaller). This shows that most of the extra stability of adding alanine in the  $\alpha$ -helical conformation rather than in the  $\beta$ -sheet conformation comes from the dipole-macro-dipole interaction, as expected. Similar results are obtained using charges for  $(\phi$

**Differential Energies between Secondary Structures**

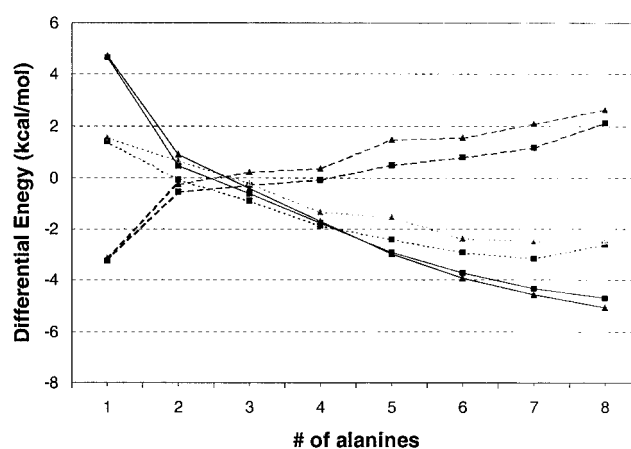


**Figure 5.** Differential energies between adding a new alanine at the N-terminus in either the  $\alpha$ -helix or  $\beta$ -sheet conformation (gas phase energy is indicated by solid line, solvation energy by dashed line, and total solution energy by dotted line; these results are also in Table 3). In each case the remaining  $N - 1$  alanines have an  $\alpha$ -helix conformation. All results from QM. Each point indicates the energy difference. The filled squares ( $\blacksquare$ ) consider the parallel  $\beta$ -sheet  $\{E[(\text{Ala})_#\text{-N}\alpha] - E[(\text{Ala})_#\text{-Np}\beta]\}$  while the filled triangles ( $\blacktriangle$ )  $\{E[(\text{Ala})_#\text{-N}\alpha] - E[(\text{Ala})_#\text{-Na}\beta]\}$  consider the antiparallel  $\beta$ -sheet. Starting with  $\# = 3$ , we see a trend in which the gas phase energy preferentially stabilizes the  $\alpha$ -helix conformation for the alanine added at the N-terminus. Here solvation retards this stability by an amount that decreases with length.

$= -120^\circ$  and  $\psi = 120^\circ)$  conformation, supporting this interpretation.

**3.1.3. Length Dependence of  $\alpha$ -Helix Stability.** Fully optimizing these structures (only with the appropriate torsional angle constraints for each residue) with QM leads to the results in Table 3 and Figure 5, which show that stabilization of an  $\alpha$ -helix conformation for alanine at the N-terminus increases with the length of the  $\alpha$ -helix. However, the incremental stabilization (Table 3b) decreases slightly with  $N$  since the distance between dipole moments increases. In solution this decrease in stability with  $N$  is quite strong because of screening by the water solvent. The solvation energy also shows this trend (Table 3 and Figure 5). The larger dipole moment of the longer  $\alpha$ -helix leads to larger solvation energies, but this screens the monodipole–macro-dipole interaction more effectively, leading to a smaller

**TABLE 3: Differential Energies for Adding a New Alanine at the N Terminus in Either the  $\alpha$ -Helix or  $\beta$ -Sheet Conformation<sup>a</sup>**

a. Differential Energies <sup>b</sup>						
	gas-phase energy		solvation energy		total solution energy	
N	$\delta(\alpha - p\beta)^c$	$\delta(\alpha - a\beta)^d$	$\delta\delta(\alpha - p\beta)^e$	$\delta\delta(\alpha - a\beta)^d$	$\delta\delta(\alpha - p\beta)^e$	$\delta\delta(\alpha - a\beta)^d$
1	4.65	4.71	-3.25	-3.15	1.40	1.55
2	0.46	0.92	-0.55	-0.24	-0.09	0.68
3	-0.61	-0.43	-0.26	0.22	-0.87	-0.20
4	-1.77	-1.70	-0.08	0.37	-1.85	-1.33
5	-2.90	-2.99	0.51	1.47	-2.39	-1.51
6	-3.71	-3.91	0.81	1.55	-2.91	-2.36
7	-4.32	-4.56	1.18	2.08	-3.14	-2.48
8	-4.71	-5.07	2.11	2.62	-2.59	-2.45

b. Change of Differential Energies ( $\delta\delta_N = \delta_N - \delta_{N-1}$ ) per Alanine Addition <sup>e</sup>						
	gas-phase energy		solvation energy		total solution energy	
N	$\delta\delta(\alpha - p\beta)$	$\delta\delta(\alpha - a\beta)$	$\delta\delta(\alpha - p\beta)$	$\delta\delta(\alpha - a\beta)$	$\delta\delta(\alpha - p\beta)$	$\delta\delta(\alpha - a\beta)$
2	-4.19	-3.79	2.70	2.91	-1.49	-0.87
3	-1.07	-1.35	0.29	0.46	-0.78	-0.88
4	-1.16	-1.27	0.18	0.15	-0.98	-1.13
5	-1.13	-1.29	0.59	1.10	-0.54	-0.18
6	-0.81	-0.92	0.30	0.08	-0.52	-0.85
7	-0.61	-0.65	0.37	0.53	-0.23	-0.12
8	-0.39	-0.51	0.93	0.54	0.55	0.03

<sup>a</sup> These results are also in Table 3. All results from QM. <sup>b</sup> Negative  $\delta$  indicates that the  $\alpha$ -helix is more stable. <sup>c</sup>  $\delta(\alpha - p\beta) = E(\alpha) - E(p\beta)$ , where the N-terminus alanine has  $\alpha$ -helical or parallel  $\beta$ -sheet conformation. <sup>d</sup>  $\delta(\alpha - a\beta) = E(\alpha) - E(a\beta)$ , where the N-terminus alanine has  $\alpha$ -helical or antiparallel  $\beta$ -sheet conformation. <sup>e</sup> Here a negative number indicates that the  $\alpha$ -helix is increasingly stabilized by the increase in length.

change of differential solvation energy (between  $\alpha$ -helix and  $\beta$ ) as the  $\alpha$ -helix length increases.

Figure 5 shows that for a single alanine (a dipeptide actually, because of the  $\text{CH}_3\text{CO}$  and  $\text{NHCH}_3$  groups added to the N- and C-terminus of an alanine, respectively), the  $\alpha$ -helical conformation is 4.6 kcal/mol *less* stable than the  $\beta$ -sheet structures in gas phase. This energy difference is reduced in water, because the solvation substantially stabilizes the  $\alpha$ -helical conformation over the  $\beta$ -sheet conformations. As a result in water the  $\alpha$ -helical conformation is 1.6 kcal/mol *less* stable than the  $\beta$  sheet conformation.

For all peptides studied, the effect of the dipole-macro-dipole interaction in solution is smaller than for the gas phase because the screening effects of solvation. However, as the length of  $\alpha$ -helices increases, the difference of the differential energies between in the gas phase and in solution decreases for the short length of  $\alpha$ -helices (when the number of alanine is less than 5) while it becomes bigger for long  $\alpha$ -helices (when the number of alanine is greater than 4).

#### 4. Discussion

It is well-known that  $\alpha$ -helices lead to dipole moments along their axes, pointing from the C-termini to the N-termini.<sup>23,24</sup> These dipole moments are developed by the appropriate alignment of both the amino and carbonyl groups of each residue in its  $\alpha$ -helical conformation, resulting a partial positive charges at the N-termini and a partial negative charges at the C-termini of  $\alpha$ -helices. Many experimental and theoretical studies have shown both the existence of these  $\alpha$ -helix dipole moments and the interactions of this  $\alpha$ -helix dipoles with dipolar or charged groups located at the end of the  $\alpha$ -helices.<sup>29-31</sup> As shown in Table 4 we also find an increased dipole with length in both gas phase and solution.

However, little attention has been paid to the interactions

**TABLE 4: Total Dipole Moment (Debye) along Axis of Helix, for the N Terminus  $\alpha$ ,  $p\beta$ , or  $a\beta$** 

a. Gas Phase					
# alanine	$\alpha$	$p\beta$	$a\beta$	a- $p\beta$	a- $a\beta$
1	6.6	2.6	2.5	4.0	4.1
2	10.0	3.3	3.0	6.7	7.1
3	14.3	6.9	6.1	7.4	8.1
4	18.3	10.7	10.2	7.6	8.1
5	22.6	14.7	14.4	7.8	8.2
6	27.4	19.3	18.7	8.1	8.7
7	32.3	24.2	23.5	8.1	8.7
8	37.0	28.9	28.4	8.1	8.6

b. Solution Phase					
# alanine	$\alpha$	$p\beta$	$a\beta$	a- $p\beta$	a- $a\beta$
1	9.2	3.4	3.3	5.9	6.0
2	13.5	4.7	4.3	8.8	9.2
3	18.5	9.0	8.2	9.5	10.3
4	23.4	13.6	13.1	9.8	10.3
5	28.2	18.4	18.1	9.8	10.1
6	33.5	23.6	23.0	10.0	10.5
7	38.9	29.0	28.3	9.9	10.6
8	44.0	34.1	33.7	9.9	10.3

occurring *within* the alanine dipoles of the  $\alpha$ -helix. Our calculations on the polyaniline peptides show that there exist substantial interactions among the dipole moments of each residue with the whole dipole moment of the  $\alpha$ -helix. These interactions help the peptides retain the  $\alpha$ -helical structure by stabilizing each residue in its  $\alpha$ -helical conformation over the  $\beta$ -sheet conformation.

These interactions can be thought of as dipole-dipole interactions between the dipole moment of each residue with the dipole moments of the remaining residues in the  $\alpha$ -helices (Figure 1). This picture is oversimplified because the distribution of local dipoles at short distances leads to important multipole-multipole contributions. Hence we refer to them as the mono-dipole-macro-dipole interactions.

To obtain reliable magnitudes for these monodipole-macro-dipole interactions, it is necessary to use peptides longer than 4 residues. For the case of two alanines (actually a tripeptide), our results show that there exists a dipole-dipole interaction between the dipole moments of each residue. In gas phase the dipole-dipole interaction stabilizes the  $(\text{Ala})_2\text{-N}\alpha$  while it destabilizes  $(\text{Ala})_2\text{-N}p\beta$  and  $(\text{Ala})_2\text{-N}a\beta$  (Table 3). In solution, however,  $(\text{Ala})_2\text{-N}\alpha$  does not gain as much stabilization as other lengths of  $\alpha$ -helices. It seems that the net effect of solvation and screening approaches zero for the case of two alanines.

These results support the conclusion that formation of the first turn of an  $\alpha$ -helix is the rate-limiting step.<sup>18</sup> Table 3 and Figure 5 suggest that until the first H-bond between alanines of  $i$  and  $i+4$  is formed, adding alanine at the amino terminus in the  $\alpha$ -helical conformation is less stable than adding it in the  $\beta$ -sheet conformations. As the  $\alpha$ -helix length extends, the dipole-macro-dipole interaction increasingly favors the alanine addition at the amino terminus in the  $\alpha$ -helical conformation as compared to a  $\beta$ -sheet conformation. This is reasonable since increasing the length of the  $\alpha$ -helix leads to increasing dipole-macro-dipole interactions that stabilizes the whole structure when the alanine at the amino terminus has the  $\alpha$ -helical conformation while the dipole-macro-dipole interaction becomes worse when the alanine at the amino terminus has the  $\beta$ -sheet conformation (Figure 1).

This explains the cooperative process in forming  $\alpha$ -helices.<sup>19-21</sup> After forming the first turn of an  $\alpha$ -helix, additional residues added to the end of the  $\alpha$ -helix stabilize the  $\alpha$ -helical conforma-

tion over the  $\beta$ -sheet conformations due to the monodipole–macro-dipole interaction.

Our results are consistent with experimental results showing dipole–dipole or charge–dipole interactions between the dipole moment of  $\alpha$ -helix and the dipolar or charged group located at the end of the  $\alpha$ -helix.<sup>25–27</sup> The experimental results also show that the first turn of  $\alpha$ -helix contributes most of the interaction (about 80% of the total) with the first two turns contribute 95%.<sup>27</sup> Figure 5 shows that in solution the monodipole–macro-dipole interactions are almost saturated at lengths of 7 or 8 while in gas phase they continue to increase as the  $\alpha$ -helices become longer.

The environment in early stages of protein folding (when the secondary structures start to form) differs from that in the final native structure. For the native protein structures almost all functional groups capable of making H-bonds are H-bonded with the neighboring functional groups and local dipole moments are neutralized by nearby dipoles. However, inside the folding protein the screening effect by neighboring residues is lower than in the water outside of proteins, leading to an environment inside the protein intermediate between the gas phase and the solution phase. In the early stage of protein folding the environment might be closer to the gas phase than to that of the native structure, because all neutralization is not yet completely established.<sup>36–38</sup> Therefore, in the early stage of protein folding to terminate an  $\alpha$ -helix requires a residue (or residues) that breaks the favorable dipole–macro-dipole (Figure 1). Thus, the terminal residue must strongly prefer a conformation substantially different than the  $\alpha$ -helix ( $\phi = -57^\circ$  and  $\psi = -47^\circ$ ). To minimize this cost in potential energy there should be a mechanism to neutralize the dipole–macro-dipole interaction. Such neutralization could be provided by charged residues, residues with polar groups and residues with high polarizability. The charged residues can neutralize the dipole moment of  $\alpha$ -helices by dipole–charge interaction. The polar residues also can neutralize it by dipole–dipole interaction or by making H-bond with any amino or carbonyl groups, which are located at the end of  $\alpha$ -helices and therefore are not involved in the  $i + 3$  H-bond of  $\alpha$ -helices.

**Acknowledgment.** This research was supported by a grant from NIH (HD36385) and completed with funding from NSF (MRI and CHE 95-22179). The facilities of the MSC are also supported by grants from DOE ASCI ASAP, ARO-MURI, NSF-MRI, NSF-CHE, BP Amoco, Chevron Corp., NASA, Beckman Institute, Seiko-Epson, Exxon, Asahi Chemical, Avery-Dennison, Dow, and 3M.

## References and Notes

- Mutz, M. W.; Case, M. A.; Wishart, J. F.; Ghadiri, M. R.; McLendon, G. L. *J. Am. Chem. Soc.* **1999**, *121*, 858.
- Clementi, C.; Carloni, P.; Maritan, A. *Proc. Natl. Acad. Sci. U.S.A.* **1999**, *96*, 9616.
- Tuchscherer, G.; Scheibler, L.; Dumy, P.; Mutter, M. *Biopolymers* **1998**, *47*, 63.
- Taylor, W. R.; Thornton, J. M. *J. Mol. Biol.* **1984**, *173*, 487.
- Finkelstein, A. V.; Reva, B. A. *Nature* **1991**, *351*, 497.
- Bowie, J. U.; Luthy, R.; Eisenberg, D. *Science* **1991**, *253*, 164.
- Jones, D. T.; Taylor, W. R.; Thornton, J. M. *Nature* **1992**, *358*, 86.
- Edwards, M. S.; Sternberg, M. J. E.; Thornton, J. M. *Protein Eng.* **1987**, *1*, 173.
- Hurle, M. R.; Matthews, C. R.; Cohen, F. E.; Kuntz, I. D.; Toumadje, A.; Johnson, W. C., Jr. *Proteins* **1987**, *2*, 210.
- Chou, P. Y.; Fasman, G. D. *Biochemistry* **1974**, *13*, 211.
- Ganier, J.; Osguthorpe, D. J.; Robson, B. *J. Mol. Biol.* **1978**, *120*, 97.
- Gibrat, J.-F.; Ganier, J.; Robson, B. *J. Mol. Biol.* **1987**, *198*, 425.
- Lim, B. I. *J. Mol. Biol.* **1974**, *88*, 857.
- Rost, B.; Sander, C. *J. Mol. Biol.* **1993**, *232*, 584.
- Benner, S. A.; Cannarozzi, G.; Gerloff, D.; Turcotte, M.; Chelvanayagam, G. *Chem. Rev.* **1997**, *97*, 2725.
- Poland, D.; Scheraga, H. A. *Theory of Helix-Coil transitions in Biopolymers*; Academic: New York, 1970.
- Lockhart, D. J.; Kim, P. S. *Science* **1992**, *257*, 947.
- Schellman, J. A. C. R. *Trav. Lab. Carlsberg* **1955**, *29*, 230.
- Young, W. S.; Brooks, C. L., III. *J. Mol. Biol.* **1996**, *259*, 560.
- Takano, M.; Takahashi, T.; Nagayama, K. *Phys. Rev. Lett.* **1998**, *80*, 5691.
- Takano, M.; Yamato, T.; Higo, J.; Suyama, A.; Nagayama, K. *J. Am. Chem. Soc.* **1999**, *121*, 605.
- Williams, S.; Causgrove, T. P.; Gilmanshin, R.; Fang, K. S.; Callender, R. H.; Woodruff, W. H.; Dyer, R. B. *Biochemistry* **1996**, *35*, 691.
- Wada, A. *Adv. Biophys.* **1976**, *9*, 1.
- Hol, W. G. J.; Van Duijnen, P. T.; Berendsen, H. J. C. *Nature* **1978**, *273*, 443.
- Sali, D.; Bycroft, M.; Fersht, A. R. *Nature* **1988**, *335*, 740.
- Aqvist, J.; Luecke, H.; Quijcho, F. A.; Warshel, A. *Proc. Natl. Acad. Sci. U.S.A.* **1991**, *88*, 2026.
- Lockhart, D. J.; Kim, P. S. *Science* **1993**, *260*, 198.
- Lazaridis, T.; Archontis, G.; Karplus, M. *Adv. Protein Chem.* **1995**, *47*, 231.
- Yang, A.-S.; Honig, B. *J. Mol. Biol.* **1995**, *252*, 351.
- Perzel, A.; Angyan, J. G.; Kajtar, M.; Viviani, W.; Rivail, J.-L.; Marcoccia, J.-F.; Csizmadia, I. G. *J. Am. Chem. Soc.* **1991**, *113*, 6256.
- Park, C.; Carlson, M. J.; Goddard, W. A., III. *J. Phys. Chem. A* **2000**, *104*, 2498.
- Ringnalda, M. N.; Langlois, M.-M.; Greeley, B. H.; Murphy, R. B.; Russo, T. V.; Cortis, C.; Muller, R. P.; Marten, B.; Donnelly, R. E., Jr.; Mainz, D. T.; Wright, J. R.; Pollar, T. W.; Gao, Y.; Won, Y.; Miller, G. H.; Goddard, W. A., III; Friesner, R. A. PS-GVB, v2.24; 1995.
- Greeley, B. H.; Russo, T. V.; Mainz, D. T.; Friesner, R. A.; Langlois, J.-M.; Goddard, W. A., III; Donnelly, R. E.; Ringnalda, M. N. *J. Chem. Phys.* **1994**, *101*, 4028.
- Tannor, D. J.; Marten, B.; Murphy, R.; Friesner, R. A.; Stikoff, D.; Nicholls, A.; Ringnalda, M.; Goddard, W. A., III; Honig, B. *J. Am. Chem. Soc.* **1994**, *116*, 11875.
- Molecular Simulations Inc., San Diego, California.
- Haynie, D. T.; Freire, E. *Proteins* **1993**, *16*, 115.
- Kuwajima, K. *FASEB J.* **1996**, *10*, 102.
- Ptitsyn, O. B. *Adv. Protein Chem.* **1995**, *47*, 83.